Macromolecular Rapid Communications
www.mrc-journal.de

Multicomponent Stress-Sensing Composites Fabricated by 3D-Printing Methodologies

*Harald Rupp and Wolfgang H. Binder**

The preparation and characterization of mechanoresponsive, 3D-printed composites are reported using a dual-printing setup for both, liquid dispensing and fused-deposition-modeling. The here reported stress-sensing materials are based on high- and low molecular weight mechanophores, including poly(ε-caprolactone)-, polyurethane-, and alkyl(C11)-based latent copper(I) bis(N-heterocyclic carbenes), which can be activated by compression to trigger a fluorogenic, copper(I)-catalyzed azide/alkyne "click"-reaction of an azide-functionalized fluorescent dye inside a bulk polymeric material. Focus is placed on the printability and postprinting activity of the latent mechanophores and the fluorogenic "click"-components. The multicomponent specimen containing both, azide and alkyne, are manufactured via a 3D-printer to place the components separately inside the specimen into void spaces generated during the FDM-process, which subsequently are filled with liquids using a separate liquid dispenser, located within the same 3D-printing system. The low-molecular weight mechanophores bearing the alkyl-C11 chains display the best printability, yielding a mechanochemical response after the 3D-printing process.

Mechanoresponsive polymers constitute an important class of materials, able to sense and visualize stress via easily recordable responses.[1] Conventionally appropriate reporter molecules or components are embedded into polymers where stress-response should be detected.[2] Various chemical stress-quantification-tools have been demonstrated by so-called mechanophores including stress-induced chemiluminescence,[3–5] the release of small molecules[6–9] and direct mechanochromic indicators.[10–18] Alternatively, the induction of catalytic reactions based on the decoupling metal–ligand complexes by mechanical stimuli is used.[19–26] The most commonly used mechanochromic polymers are based on spiropyranes,[16,18] able to generate a merocyanine chromophores upon mechanical activation depending on their substitution pattern. Especially the NO_2-functionalized dyes manifest in an intense purple color, finally allowing to quantify the exerted stress within the material.[10,27–31] Therefore, in view of the multicomponent-nature of such polymeric materials the use of 3D-printing methodologies is attractive, allowing to place components for the direct stress-detection as well as additional reporter molecules required for the quantification of stress into the same material.[32,33]

A novel and efficient methodology for stress-detection uses mechanophores directly activated by metal/ligand cleavage, coupled to a subsequent catalytic reaction of the then freed metal-coordination-site.[22,24,26,34] The catalysts used to this endeavor in our group are based on copper(I) bis(*N*-heterocyclic carbene) mechanocatalysts, connected to a fluorogenic copper-azide-alkyne "click" reaction (CuAAC) of 3-azido-7-hydroxycoumarin with phenylacetylene. Both components are nonfluorescent before mechanochemical activation, but react to a fluorescent dye to visualize applied stress on the polymer backbone induced via sonication, grinding, or tensile/compression forces.[35–37]

We here report on a novel 3D-print method to manufacture a stress-responsive polymer, based on microsized capsules, embedded into a thermoplastic polymer matrix by combining different 3D-printing techniques. The approach aims to generate functional composite materials based on mixing a polymer (poly(caprolactone), PCL) with different Cu-based-mechanophores (**1a**, **1b**, **1c**) and 3-azido-7-hydroxycoumarin to create microsized capsules during 3D-printing, filled with phenylacetylene (**Figure 1**) as the second reactive component for the fluorogenic "click"-reaction. The 3D-printing method aims to directly dispense the liquid into a solid matrix during the FDM-printing process, thus largely suppressing a primordial thermal activation of the "click" reaction during 3D-printing.[38]

The first step in the chemical design constituted the synthesis of a suitable mechanophore, able to be 3D-printed under preservation of its stress-reporting function. To this endeavor, we have prepared the copper(I)-bis(NHC)-mechanophores **1a**, **1b**, **1c** (see **Figure 2**), where either a C11-chain (**1a**), a PCL-chain (**1b**), or an urethane (**1c**) are attached to the bis-*N*-heterocyclic-carbene (NHC)-Cu(I)-complexes as the active, mechanoresponsive elements. Synthesis was accomplished by quaternization reaction of telechelic bromo-functionalized C_{11}- and short PCL-chains

H. Rupp, Prof. W. H. Binder
Chair of Macromolecular Chemistry
Division of Technical and Macromolecular Chemistry
Institute of Chemistry
Faculty of Natural Sciences II (Chemistry, Physics and Mathematics)
Martin Luther University Halle-Wittenberg
von-Danckelmann-Platz 4, Halle D-06120, Germany
E-mail: wolfgang.binder@chemie.uni-halle.de

The ORCID identification number(s) for the author(s) of this article can be found under https://doi.org/10.1002/marc.202000450.

DOI: 10.1002/marc.202000450

Macromolecular Rapid Communications
www.mrc-journal.de

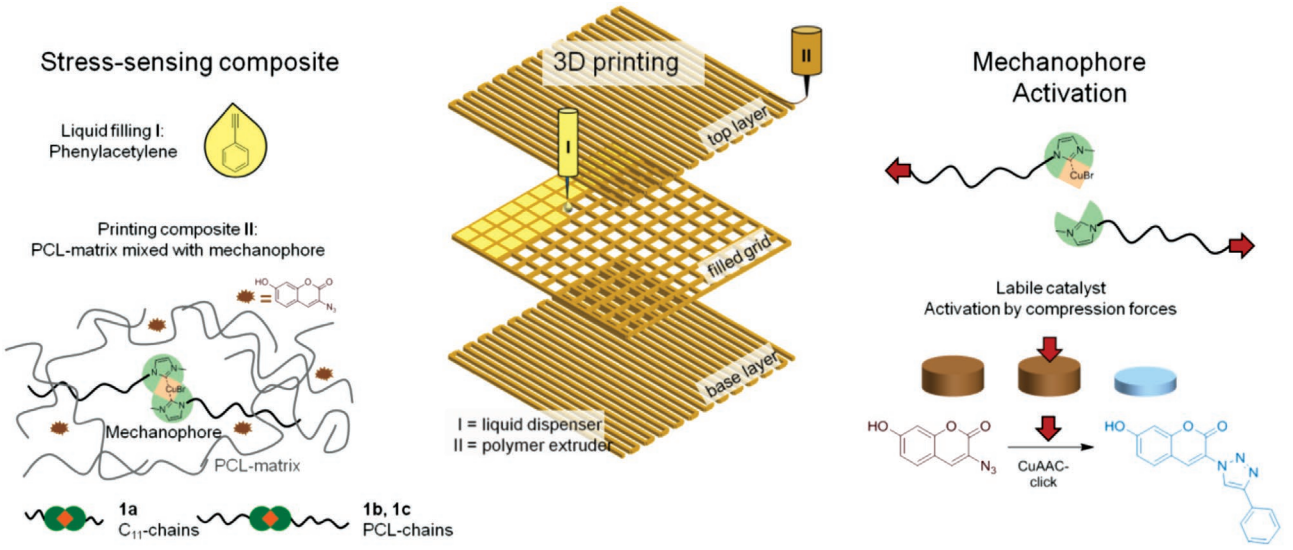

Figure 1. Concept for the 3D-printing of multicomponent-polymers containing the copper(I)-bis(NHC)-mechanophores based on C11-chains (**1a**) and poly(*ε*-caprolactone) (**1b**, **1c**), successfully embedded into 3D-printable PCL together with a fluorogenic dye. The second reaction component (phenylacetylene) (liquid filling I)) was added as a liquid into 3D-printed voids by direct dispensing. 3D-printed specimens were tested with compression cycles for their catalytic activity of the "CuAAC-click" reaction.

(M_w = 1800 Da) to yield the 1-methylimidazolium bromide functionalized chains, followed by conversion of the 1-methylimidazole-chains to the respective copper(I)-bis(NHC)-mechanophores with Cu_2O-powder (5 µm). To check for eventual side-reactions during the Cu_2O-treatment, hydroxy-functionalized PCL–OH was treated with the same reaction conditions, detecting no side-reactions (e.g., oxidation or degradation) between pure PCL and Cu_2O via ^{1}H-NMR measurements (Figure S3, Supporting Information). The synthesis and conversion of all of the reaction steps were easily detectable in ^{1}H-NMR. The bromo-functionalized PCL (**Figure 3**a) showed the expected signals for the CH_2-Br-functionality at 3.39 ppm (t, J = 6.9 Hz, 2H). After quaternization reaction new signals for the 1-methylimidazolium bromide function appeared. The NHC-proton signal was detected at 10.76 ppm (s, 1H) besides the aromatic bonds at 7.25 ppm (s, 1H) and 7.21 ppm (s, 1H), also for the CH_2-group 4.34–4.28 (m, 2H), and the methyl group at 4.12 (s, 3H) (Figure 3b).

The last reaction step, the conversion to the copper(I)-bis(NHC)-mechanophore, resulted in the PCL polymer containing the desired product as judged by NMR via resonances at 6.14 ppm (dd, J = 7.0, 2.8 Hz, 4H), 3.66–3.54 (m, 8H), and 3.23 (s, 6H) (Figure 3c), generated in an acceptable yield for the final mechanophore **1b** of 32%. The conversion to the 1-methylimidazolium bromide functionalized chains were supported by matrix assisted laser desorption (MALDI)-ToF-mass spectrometry (MS) measurements, showing all details for the reactions as proven by MALDI-TOF (see Figure S1, Supporting Information), indicating the desired MS-spectra and isotopic patterns for all intermediates. Proof for the formation of the mechanophore **1b** could be obtained by size exclusion chromatography (SEC), resulting in a doubling of the molecular weight in the bis-Cu(I)-NHC-complex in comparison to the starting-polymers as checked via SEC-measurements in THF (**Figure 4**). Using the calibration for polystyrene-standards (300–170 000 g mol^{-1}) the following shifts were measured in SEC: PCL-Br (M_n = 3800, M_w = 5100, PDI = 1.3) versus PCL-M **1b** (M_n = 7600, M_w = 11 000, PDI = 1.4). Mechanophore **1c**, based on an chain extension via hexamethylenediisocyanate (HDI) was prepared according to previously reported methodologies[25] by reaction of the C11-mechanophore **1a** with hexamethylene diisocyanate (HDI, molar ration **1a**/HDI = 1:30).

3D-printing was accomplished using PCL as the base matrix (PCL (M_w = 45 kDa)), embedding the required components directly during the printing process. The printer, a regenHU

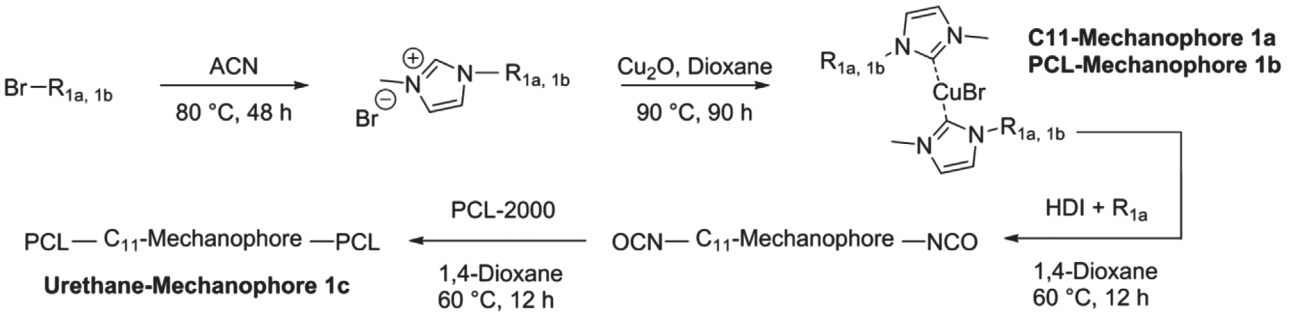

Figure 2. Reaction schema for the synthesis of different copper(I)-bis(NHC)-mechanophores **1a** (C11), **1b** (PCL-M), and **1c** (Urethane-M).

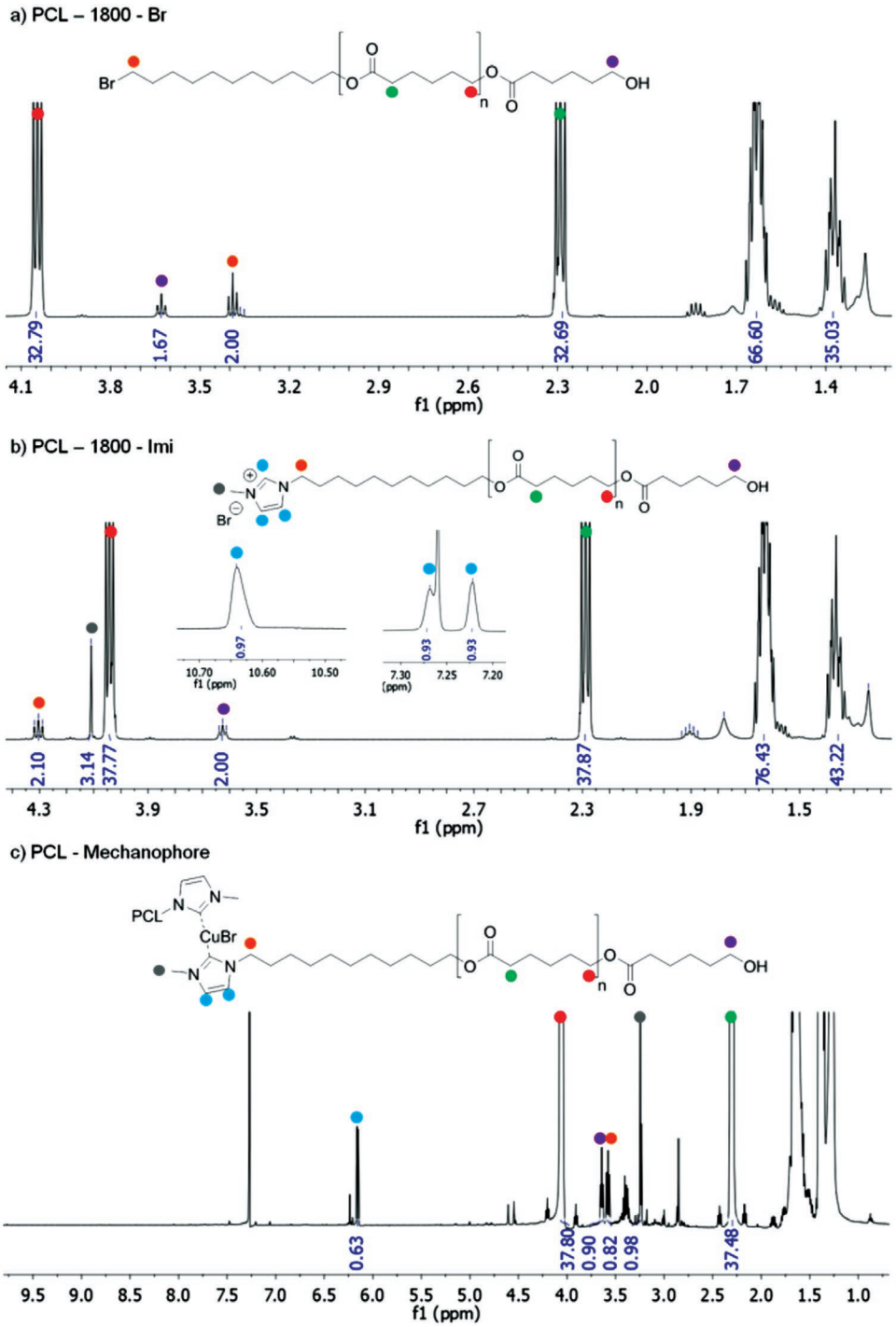

Figure 3. ^{1}H-NMR analyses of the different modification steps for the PCL-mechanophore **1b.** Synthesis via PCL-Br a), PCL-Imi b), and the PCL-copper(I)-bis(NHC)-mechanophore c).

3D Discovery, equipped with a heatable polymer extrusion printing head with a metal nozzle, was used for printing of the polymer composites. First, the printed composites were based on PCL as matrix-polymer containing 1 wt% coumarin-azide (5×10^{-5} mmol mg^{-1} matrix) with a corresponding amount of the mechanophore **1a**, **1b**, or **1c** (5×10^{-6} mmol mg^{-1} matrix) directly mixed into it.

Similar to a procedure recently developed in our research group,[38] a 3D-printed structure with a square-shaped base of 5 × 5 mm and a grid with gaps of around 300 µm were designed in a BioCAD program. First the two layers of the 100% filled base area were printed using fused deposition modeling (FDM) for the PCL composite. Subsequently, two layers of the grid structure, forming the 3D-printed capsules, were printed on

Macromolecular Rapid Communications
www.mrc-journal.de

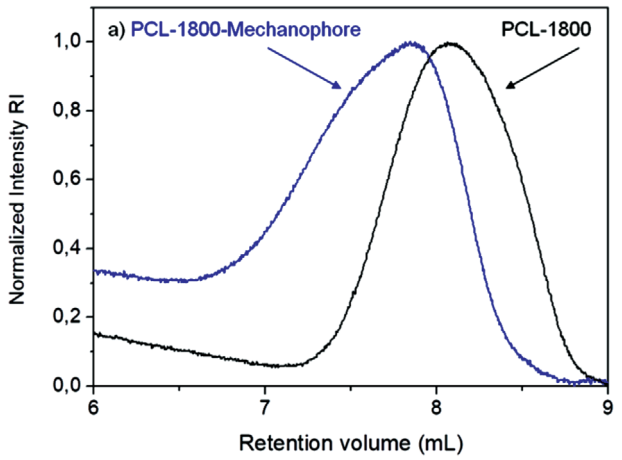

Figure 4. SEC data of the initial PCL-Br polymer and the final PCL-mechanophore **1b** with a percentage content of 32%.

top. In between, the second printing head dispensed phenylacetylene into the created gaps by drop-on-demand jetting, completely filling the voids. The top closing layers consisted of two completely filled composite layers, again printed by FDM (results in **Figure 5**a,b). The temperature of the printing nozzle was adjusted to 70–80 °C according to the rheology data, with the temperature of the tank of the printing head set 10 °C higher than the temperature of the printing nozzle.

The composites were printed on a standard glass slide equipped with a masking tape for mechanical adhesion. Based on the rheology data of our previous publication[39] and the known 3D-printing window of the here used 3D printer (η = 200–2000 Pa s, γ = 10–30 s^{-1}, ϑ = 30–240 °C), PCL polymers with an intermediate molecular weight can be printed. The influence of the mechanophores **1a**, **1b**, **1c** (catalytic amounts, amounts see **Table 1**) and the fluorogenic dye (1 wt%) on the rheological properties of matrix was negligible compared to the pure PCL matrix (Figure S2, Supporting Information). PCL (45 kDa) showed a viscosity range of 700–360 Pa s while changing the temperature from 70 to 90 °C, leading to an excellent extrusion and easy to handle printing properties (Figure S2, Supporting Information). A very uniform polymer strand could be extruded at 80 °C, which solidified in a reasonable time range of 5–10 s. Subsequently the drop-on-demand liquid printing head was set to one drop per grid hole at room temperature. The 3 mL cartridge was filled with phenylacetylene and pressed with air of 0.01–0.04 MPa to move the liquid through the inkjet nozzle and deposit 2.5 µL phenylacetylene into the void (Figure 5a,b).

The printing composites were analyzed via ^{1}H-NMR after heating and extrusion, checking for the presence of the copper(I)-bis(NHC) signal (6.15 ppm, dd, 4H) after the extrusion-process of the 3D-printing. Only the mechanophore with C_{11}-chains (**1a**) did outlast the printing conditions. Both, PCL-mechanophore (**1b**) and urethane-mechanophore (**1c**), did not survive the extrusion, since no signal for the copper(I)-bis(NHC)-moieties could be detected (Figure S4, Supporting Information). Subsequently both, the mold-prepared and the 3D-printed samples, (for preparation see Supporting Information) were analyzed for their

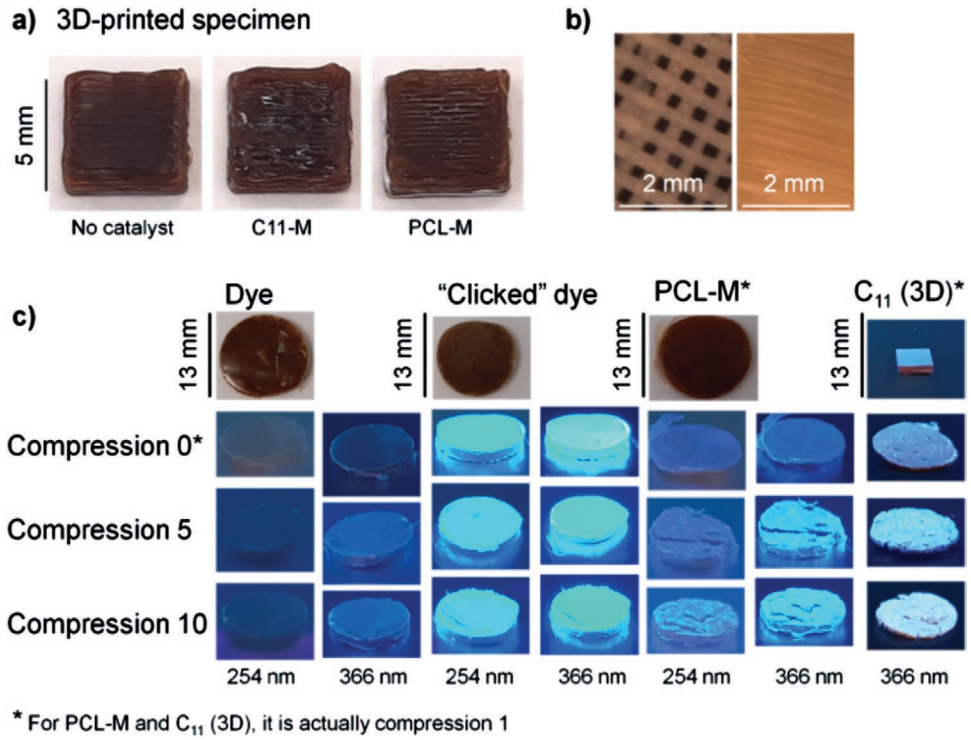

Figure 5. Pictures of the 3D-printed specimen with different composites prepared by using a dual-head 3D-printer. a) Microscopic images of an emptied inner grid structure and the top closing layer. b) Photos of mold-casted samples after compression cycles under normal light and UV–light (254 + 366 nm) showing the increase in fluorescence activity after compression force was applied. c) The samples refer to pure dye samples of the calibration curve determination (dye and "clicked" dye), as well as PCL-M (Table 1, Entry III) and C11-M (3D) (Table 1, Entry VI).

Table 1. The different materials of mold-casted and 3D-printed (3D) composites including different mechanophore catalysts 1a, 1b, 1c are listed (calculated for 99% purity), as well as the final catalytic activity of each mixture.

Entry	Sample[a)] [mg g_{Matrix}^{-1}]	Mechanophore [mg g_{Matrix}^{-1}]	Coumarin dye [µL]	Phenyl acetylene	Catalytic activity Δ[b)] [%]
I	No catalyst	–	10	2.5	0.34
II	C11-M (1c)	2	10	2.5	0.62
III	PCL-M (1a)	12	10	2.5	0.98
IV	Urethane-M (1b)	13	10	2.5	1.67
V	None (3D)	–	10	2.5	0.47
VI	C11-M (3D) (1c)	2	10	2.5	0.51

[a)]The samples entry I–IV were prepared by mold-casting method (Supporting Information), samples V–VI were manufactured by 3D-printing; [b)]For the solid state measurements the sample was fixed between two glass slides and the reflected fluorescence was detected. For each sample the measurements were done for both sides. After calibration, the fluorescence intensity was calculated to yield the "click"-reaction yield.

mechanophore activity by a combination of compression cycles and subsequently measured by solid state fluorescence measurements, indicative for the fluorogenic "click"-reaction. With solid state fluorescence reflection measurements as well as images under UV–light the change in fluorescence intensities were measured/visualized (Figures 5 and 6). For calibration of the system see Figure S5 (Supporting Information). The sample with no mechanophoric catalyst showed only minor activation of the fluorogenic dye of ≈0.3% for the molded sample (Entry I) and ≈0.5% for the 3D-printed sample (Entry V), presumably by thermal activation during the printing process. The C_{11}-mechanophore (**1a**) samples showed catalytic activities of ≈0.6% (mold, entry II) and ≈0.5%, respectively (3D-printed, entry VI). The higher fluorescence intensity for the C_{11} (3D) sample was due to the thermal "click-reaction" occurring during the final FDM process, where hot printing composite gets in direct contact with phenylacetylene. For the PCL-based mechanophores only the molded samples could be measured. The samples showed activities of ≈1.0% (PCL-M, entry III) and ≈1.7% (urethane-M, entry IV). The 3D-printing of the labile copper(I)-bis(NHC)-bond could be achieved, still retaining at least parts of its active form keeping the copper(I)-bis(NHC)-bonds intact, whereas the larger mechanphores based on the PCL-mechanophore **1b** and the urethane-mechanophore **1c** did not withstand the printing conditions. Presumably, their easier activation during extrusion in view of their increased chain length is responsible for this observation.

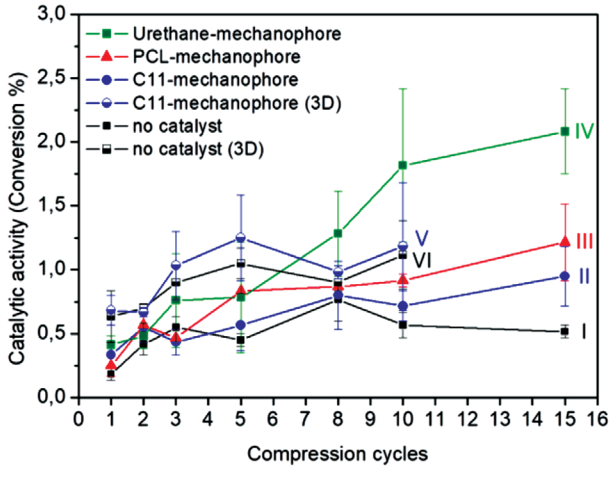

Figure 6. Catalytic activity of different mechanophore composites (no catalyst, C11-mechanophore (**1a**), PCL-mechanophore (**1b**), urethane-mechanophore (**1c**)) using repeated compression cycles to activate the copper(I)-bis(NHC)-mechanophores.

In conclusion, the 3D-printing of copper(I)-bis(NHC)-mechanophores was investigated using a multicomponent-printed-system, generating polymer-composites with stress-detecting properties. As demonstrated here the printing-results and final activities of the three different mechanophores strongly depended on the chain length used under the 3D-printing conditions of 80 °C. Whereas short chain mechanophores with side chains of C_{11} (**1a**) can easily be mixed with the printable PCL polymer and subsequently be extruded retaining their mechanophoric activity, the higher molecular weight mechanophores (**1b**, $M_{w,\ PCL\text{-}M}$ = 1800 Da, and **1c**, $M_{w,\ Urethane\text{-}M}$ = 2000 Da) could not be 3D-printed, although both showed catalytic activity (1.0–1.7%) in compression force cycles when produced by a mold casting method, comparable to previous results.[26] Thus, the reported methodology can be advantageous for the fabrication of multilayer-polymers, where the stress-reporting tool is placed in a specific part of the polymeric-specimen where stress-detection is required, keeping all other parts of the polymer structurally native. We think that this methodology can be advantageous when integrated into production-techniques where 3D-printing technology is already established.

Supporting Information

Supporting Information is available from the Wiley Online Library or from the author.

Acknowledgements

The authors thank the Leistungszentrum "System- und Biotechnologie" (Uni-CBS1) for financial support for the project "Biologisch abbaubare Partikel über Enkapsulierungsmethoden: Emulsions-/Evaporationsverfahren und 3D-Printing". They also thank the EU-BAT-4-ever-project within the Horzon-2020 grant agreement no. 957225 for financial support.

Open access funding enabled and organized by Projekt DEAL.

Conflict of Interest

The authors declare no conflict of interest.

Keywords

3D-printing, Cu-N-heterocylic-carbene-complexes, fluorogenic click-chemistry, mechanophores, synthesis

Received: August 15, 2020
Revised: September 23, 2020
Published online: October 13, 2020

[1] S. Schrettl, D. W. R. Balkenende, C. Calvino, M. Karman, A. Lavrenova, L. N. Neumann, Y. Sagara, E. Verde-Sesto, M. di Giannantonio, Y. C. Simon, K. M. Fromm, M. Lattuada, C. Weder, *CHIMIA* **2019**, *73*, 7.
[2] R. G. Omar, A. Edward, B. Livia, B. Nico, *Adv. Mater.* **2018**, *30*, 1705483.
[3] Y. Chen, A. J. H. Spiering, S. Karthikeyan, G. W. M. Peters, E. W. Meijer, R. P. Sijbesma, *Nat. Chem.* **2012**, *4*, 559.
[4] Y. Chen, R. P. Sijbesma, *Macromolecules* **2014**, *47*, 3797.
[5] J. M. Clough, R. P. Sijbesma, *ChemPhysChem* **2014**, *15*, 3565.
[6] C. E. Diesendruck, B. D. Steinberg, N. Sugai, M. N. Silberstein, N. R. Sottos, S. R. White, P. V. Braun, J. S. Moore, *J. Am. Chem. Soc.* **2012**, *134*, 12446.
[7] M. B. Larsen, A. J. Boydston, *J. Am. Chem. Soc.* **2013**, *135*, 8189.
[8] M. B. Larsen, A. J. Boydston, *J. Am. Chem. Soc.* **2014**, *136*, 1276.
[9] G. R. Gossweiler, G. B. Hewage, G. Soriano, Q. Wang, G. W. Welshofer, X. Zhao, S. L. Craig, *ACS Macro Lett.* **2014**, *3*, 216.
[10] S. L. Potisek, D. A. Davis, N. R. Sottos, S. R. White, J. S. Moore, *J. Am. Chem. Soc.* **2007**, *129*, 13808.
[11] D. W. R. Balkenende, S. Coulibaly, S. Balog, Y. C. Simon, G. L. Fiore, C. Weder, *J. Am. Chem. Soc.* **2014**, *136*, 10493.
[12] K. R. Fitch, A. P. Goodwin, *Chem. Mater.* **2014**, *26*, 6771.
[13] Y. Sagara, K. Kubo, T. Nakamura, N. Tamaoki, C. Weder, *Chem. Mater.* **2017**, *29*, 1273.
[14] Y. Sagara, M. Karman, E. Verde-Sesto, K. Matsuo, Y. Kim, N. Tamaoki, C. Weder, *J. Am. Chem. Soc.* **2018**, *140*, 1584.
[15] T. Watabe, K. Ishizuki, D. Aoki, H. Otsuka, *Chem. Commun.* **2019**, *55*, 6831.
[16] M. Sommer, H. Komber, *Macromol. Rapid Commun.* **2013**, *34*, 57.
[17] L. Metzler, T. Reichenbach, O. Brügner, H. Komber, F. Lombeck, S. Müllers, R. Hanselmann, H. Hillebrecht, M. Walter, M. Sommer, *Polym. Chem.* **2015**, *6*, 3694.
[18] M. Raisch, D. Genovese, N. Zaccheroni, S. B. Schmidt, M. L. Focarete, M. Sommer, C. Gualandi, *Adv. Mater.* **2018**, *30*, 1802813.
[19] A. Piermattei, S. Karthikeyan, R. P. Sijbesma, *Nat. Chem.* **2009**, *1*, 133.
[20] R. T. M. Jakobs, R. P. Sijbesma, *Organometallics* **2012**, *31*, 2476.
[21] R. T. M. Jakobs, S. Ma, R. P. Sijbesma, *ACS Macro Lett.* **2013**, *2*, 613.
[22] P. Michael, W. H. Binder, *Angew. Chem., Int. Ed.* **2015**, *54*, 13918.
[23] P. Michael, S. K. Sheidaee Mehr, W. H. Binder, *J. Polym. Sci., Part A: Polym. Chem.* **2017**, *55*, 3893.
[24] S. Funtan, P. Michael, W. H. Binder, *Biomimetics* **2019**, *4*, 24.
[25] M. Biewend, P. Michael, W. H. Binder, *Soft Matter* **2020**, *16*, 1137.
[26] P. Michael, M. Biewend, W. H. Binder, *Macromol. Rapid Commun.* **2018**, *39*, 1800376.
[27] B. A. Beiermann, S. L. B. Kramer, J. S. Moore, S. R. White, N. R. Sottos, *ACS Macro Lett.* **2012**, *1*, 163.
[28] M. Li, Q. Zhang, S. Zhu, *Polymer* **2016**, *99*, 521.
[29] T. A. Kim, M. J. Robb, J. S. Moore, S. R. White, N. R. Sottos, *Macromolecules* **2018**, *51*, 9177.
[30] M. Li, Q. Zhang, Y.-N. Zhou, S. Zhu, *Prog. Polym. Sci.* **2018**, *79*, 26.
[31] A.-D. N. Celestine, N. R. Sottos, S. R. White, *Strain* **2019**, *55*, e12310.
[32] I. Peterson Gregory, M. Yurtoglu, B. Larsen Michael, L. Craig Stephen, A. Ganter Mark, W. Storti Duane, J. Boydston Andrew, *Rapid Prototyping J.* **2015**, *21*, 520.
[33] G. I. Peterson, M. B. Larsen, M. A. Ganter, D. W. Storti, A. J. Boydston, *ACS Appl. Mater. Interfaces* **2015**, *7*, 577.
[34] W. H. Binder, *Polymer* **2020**, *202*, 122639.
[35] C. Calvino, L. Neumann, C. Weder, S. Schrettl, *J. Polym. Sci., Part A: Polym. Chem.* **2017**, *55*, 640.
[36] J. N. Brantley, K. M. Wiggins, C. W. Bielawski, *Polym. Int.* **2013**, *62*, 2.
[37] S. Neumann, M. Biewend, S. Rana, W. H. Binder, *Macromol. Rapid Commun.* **2020**, *41*, 1900359.
[38] H. Rupp, W. H. Binder, *Adv. Mater. Technol.*, https://doi.org/10.1002/admt.202000509.
[39] H. Rupp, D. Döhler, P. Hilgeroth, N. Mahmood, M. Beiner, W. H. Binder, *Macromol. Rapid Commun.* **2019**, *40*, 1900467.